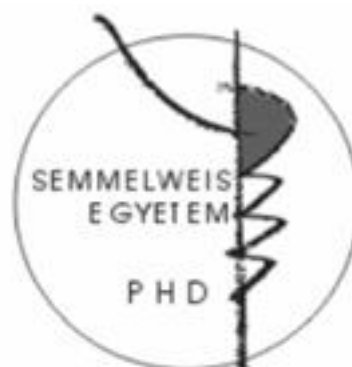


Examination of Thyrotropin-Releasing Hormone (TRH)-synthesizing System in the Rodent Hypothalamus

Ph.D. Thesis

Andrea Kádár

Semmelweis University
János Szentágothai Ph.D. School of Neuroscience



Tutor: Csaba Fekete D.Sc.

Opponents: Dóra Reglődi D.Sc.
Alán Alpár Ph.D.

Chairman of committee:	György M. Nagy D.Sc.
Members of committee:	Katalin Halasy D.Sc.
	Zsuzsa Várnainé Tóth Ph.D.

Budapest
2014

Introduction

The hypophysiotropic thyrotropin-releasing hormone (TRH) producing neurons are the main central regulators of the hypothalamus-pituitary-thyroid (HPT) axis. These neurosecretory neurons are located in the hypothalamic paraventricular nucleus (PVN) and their axons terminate outside the blood-brain barrier (BBB) in the external zone of the median eminence (ME) where TRH is secreted to the circulation. TRH stimulates the thyroid stimulating hormone (TSH) production of thyrotrop cells in the anterior pituitary that stimulates the hormone production of thyroid gland. Thyroid hormones have widespread effects including the regulation of energy metabolism by influencing the basal metabolic rate, adaptive thermogenesis and feeding behavior and regulation of the development and normal functioning of the central nervous system (CNS).

The PVN can be divided into two main divisions named based on the size of their neurons: the parvocellular and magnocellular divisions. In rats, the parvocellular division can be further divided into six subdivisions: the anterior, medial, dorsal, periventricular, ventral and lateral subdivisions. TRH-synthesizing neurons can be found in all parvocellular subdivisions in rats, but the hypophysiotropic TRH neurons are located exclusively in the periventricular and medial parvocellular subdivisions. In rats, a characteristic feature of the hypophysiotrophic TRH neurons is their cocaine- and amphetamine regulated transcript (CART) expression as this peptide was not identified in any other TRH-expressing populations of the brain. Although the localization of the hypophysiotropic TRH neurons is precisely determined in rats, limited information is available currently about the distribution of these neurons in mice, the most frequently used animal model of the current days.

Thyroid hormones regulate the TRH synthesis of hypophysiotropic neurons by negative feedback regulation. OATP1C1, the predominant thyroid hormone transporter molecule through the BBB is highly specific for thyroxine (T4), but not for triiodothyronine (T3), the active form of thyroid hormones. Therefore, local type 2 deiodinase (D2) mediated conversion of T4 to T3 is the primary source of T3 in the brain. In the hypothalamus, D2 is predominantly located in tanycytes, a specialized glial cell type lining the wall and the floor and lateral walls of the third ventricle. While the cell bodies of these cells are located in the ependymal layer, their long basal process projects to the neuropil of the arcuate, ventromedial and dorsomedial nuclei or to the capillary loops in the external zone of the median eminence (ME). The perikarya of hypophysiotropic TRH neurons are located far from the tanycytes, therefore, volume transmission between the tanycytes and the TRH neurons would be a

relatively slow process. In contrast, the tanycyte end feet processes and the terminals of the TRH neurons are closely associated in the external zone of the ME. Therefore, we hypothesized that T3 produced by tanycytes may be taken up by axon terminals of these neurosecretory neurons in the ME and transported retrogradely to the nucleus of these cells. The presence of the main neuronal thyroid hormone transporter, MCT8, in the axon terminals of hypophysiotropic neurons would confirm this hypothesis.

The hormone production of hypophysiotropic TRH neurons is strongly regulated by leptin, an adipose tissue derived satiety hormone. The effect of leptin on TRH neurons is mediated by two neuron populations of arcuate nucleus (ARC): the anorexigenic α -MSH/CART neurons which stimulate TRH expression and the orexigenic AGRP/NPY neurons which have inhibitory effect on TRH transcription. During fasting α -MSH/CART neurons are inhibited and AGRP/NPY neurons are stimulated. Interestingly, two hours after the start of refeeding α -MSH/CART neurons are active and acutely stimulate the neurons in the ventral parvocellular part of the PVN (vPVN), but TRH neurons seem to be resistant against the stimulatory effect of these neurons during the early phase of refeeding. Since leptin is able to induce the rearrangement of the synaptic inputs of some hypothalamic neuronal groups and also influence the axonal growth during development we hypothesized that the lack of leptin during fasting may result in synaptic plasticity in the arcuate-paraventricular pathway that may contribute to the melanocortin-resistance of TRH neurons during the early phase of refeeding.

c-Fos immunolabeling is often used for the determination of activated neuronal elements. Since c-Fos labeling is located in the nucleus, the characterization of the neuronal inputs of the activated neurons is difficult at light microscopic level due to the lack of the cytoplasmic labeling in these cells. The Nissl-staining method which is based on the interaction of basic dyes and the nucleic acid content of cells labels both the nucleus and the cytoplasm of neurons. However, after immunolabeling procedure, Nissl-dyes often visualize only the cell nuclei or provide only faint cytoplasmic labeling that makes the combination of immunocytochemistry and Nissl-staining less valuable. We hypothesized that the lack of cytoplasmic labeling after immunocytochemical processes is caused by the digestion of the RNA content of tissues by RNase enzyme contamination and therefore the application of RNase-free conditions and RNase inhibitors during the immunocytochemical processes could improve the labeling of cytoplasm by Nissl-staining.

Specific aims

1. To map the distribution of hypophysiotropic TRH neurons in the mouse hypothalamus
2. To determine the route of T3 transport between the thyroid hormone activating tanycytes and the hypophysiotropic TRH neurons
3. To clarify the mechanism of the melanocortin resistance of the hypophysiotropic TRH neurons during refeeding
4. To develop an improved method for the combined use of immunocytochemistry and Nissl-staining

Materials and methods

Animals

In the experiments adult male Wistar rats and adult male CD1 and TRH/Cre-Z/EG mice were used. The animals were housed under standard environmental conditions (light between 6:00 A.M. and 6:00 P.M., temperature 22°C, food and water *ad libitum*) in the animal facility of the Institute of Experimental Medicine of the Hungarian Academy of Sciences. All experimental protocols were reviewed and approved by the Animal Welfare Committee at the Institute of Experimental Medicine of the Hungarian Academy of Sciences and carried out in accordance with legal requirements of the European Community.

Methods used for mapping the distribution of hypophysiotropic TRH neurons in the PVN of mice

Fluoro-Gold injection

For the identification of hypophysiotropic neurons, four mice received intravenous injection of Fluoro-Gold. Two days later, the mice were injected intraperitoneally with same dose of Fluoro-Gold to further enhance the labeling in the hypophysiotropic cell bodies.

Single-, double- and triple labeling immunocytochemistry

Intracerebroventricular colchicine treatment was applied to facilitate the detection of the perikarya of the TRH-immunoreactive (-IR) neurons. Next day, the mice were perfused with a mixture of 4% acrolein and 2% paraformaldehyde (PFA). 25 µm thick sections were made with freezing microtome. The sections were pretreated for immunocytochemistry. The following immunocytochemical labelings were done:

1. Single labeling immunocytochemistry for mapping the distribution of TRH-IR neurons in the PVN of mice. The TRH-immunoreactivity was visualized by Ni-DAB developer. The sections were examined with brightfield microscope.
2. Triple-labeling immunofluorescence for the detection of the co-localisation of Fluoro-Gold and TRH and for the discrimination between the parvocellular TRH neurons and the magnocellular vasopressin- (AVP) or oxytocin (OT) neurons. The sections were treated with anti-TRH serum mixed with one of the following antisera: anti-Fluoro-Gold antiserum and anti-AVP or anti-OT antibodies. Then the TRH-immunoreactivity was visualised with Alexa 555-conjugated anti-sheep IgG, the AVP or OT was labeled with FITC conjugated anti mouse IgG and the Fluoro-Gold-immunoreactivity was detected with Cy5-conjugated streptavidin after application of biotinylated anti-rabbit IgG, avidin-biotin-peroxidase complex (ABC) and biotinylated tiramide (BT). For the identification of brain nuclei and subnuclei, DAPI counterstaining was performed. The sections were studied with epifluorescent and laser scanning confocal microscopes.
3. Double labeling immunofluorescence for the examination of the colocalisation of TRH and CART in the PVN of mice. The sections were treated with a mixture of sheep anti-TRH serum and mouse monoclonal anti-CART antibodies. Then the TRH-immunoreactivity was visualised with Alexa 555-conjugated anti-sheep IgG, while the CART labeling was detected with FITC-conjugated anti-mouse IgG. DAPI counterstaining was performed to facilitate the localization of the labeled neurons. The sections were examined with epifluorescent and laser scanning confocal microscopes.

Methods for determination of the potential route of T3 transport between the thyroid hormone activating tanycytes and the hypophysiotropic TRH neurons

The following immunocytochemical labelings were performed for the detection of the thyroid hormone transporter molecule, MCT8 in the hypophysiotropic axon terminals:

1. Immunocytochemistry for the light microscopic, brightfield examination of the localization of MCT8 in the median eminence. Acrolein (4%) + PFA (2%) fixed sections from mice were pretreated for immunocytochemistry as described above and labeled with anti-MCT8 rabbit polyclonal serum. The MCT8-immunoreactivity was visualized with Ni-DAB developer and the result was intensified with the Gallyas method. Images of the sections were taken with brightfield microscope.
2. Ultrastructural examination of the MCT8-IR structures in the median eminence. Coronal, 30-50µm thick sections containing the median eminence were prepared with vibratome from

rat brains fixed with a mixture of 4% acrolein and 2% PFA. After the pretreatments, the sections were incubated in rabbit anti-MCT8 serum. The MCT8 immunolabeling was detected with Ni-DAB developer and intensified with Gallyas method. The sections were embedded in Durcupan resin and ultrathin sections were cut and collected on formvar-coated single slot grids. The ultrathin sections were examined using transmission electron microscope.

3. Double-labeling immunofluorescence for the detection of MCT8 and TRH in the median eminence. Sections of rat brains fixed with 4% acrolein and 2% PFA were pretreated for immunocytochemistry. Then the sections were incubated in a mixture of anti-MCT8 and anti-TRH sera. The MCT8-immunoreactivity was visualised with Alexa555-conjugated anti-rabbit IgG while TRH was detected with FITC conjugated anti-sheep IgG. The sections were examined with laser scanning confocal microscope.

Methods used for studies focusing on the mechanism of the melanocortin resistance of the hypophysectomized TRH neurons during refeeding

The double-transgenic TRH/Cre-Z/EG indicator mice were divided into 5 groups: 1) mice fed with standard rodent chow (n=5) 2) fasted for two days (n=5) 3) fasted for two days and refed for 2 hours (n=3) 4) fasted for two days and refed for 24 hours (n=3) 5) received subcutaneous infusion of leptin (12µg/day, for 2 days) with osmotic minipump during the two days of fasting (n=3). At the end of the experiment, the animals were perfused with 4% PFA and 25µm thick coronal sections containing the PVN were prepared from the brains. After the pretreatment for immunocytochemistry the sections were incubated in a mixture of antibodies against α -MSH (produced in sheep), AGRP (rabbit) and GFP (mouse). The anti- α -MSH antibody was detected with Alexa555-conjugated anti-sheep IgG, the AGRP-labeling was detected with biotinylated anti-rabbit IgG followed by a signal amplification with ABC and DAB and incubation in Cy5-conjugated streptavidin, the GFP signal was labeled with FITC-conjugated anti-mouse IgG.

Method for combination of immunocytochemistry and Nissl-staining

For the induction of c-Fos-immunoreactivity in the vPVN, rats were fasted for three days and refed for two hours before the perfusion with 4% PFA. Two groups of sections from the brains were labeled with the same antibodies against c-Fos (detected with Ni-DAB) and NPY (visualized with DAB) and counterstained with Cresyl-violet. The difference between the two groups was that the first group was treated with standard immunocytochemical materials while the second group was treated under strictly RNase-free conditions.

Results

Mapping the distribution of hypophysiotropic TRH neurons in the mouse hypothalamus

The organization of PVN in mice

As we observed that the organization of the mouse PVN is highly different from the organization of the PVN in rats, instead of using the nomenclature of the mouse brain atlas by Paxinos and Franklin that was adapted from the rat brain nomenclature, we have divided the PVN into five parts. These parts are as follows:

- compact = a cell dense region in the mid level of PVN that contains both magno- and parvocellular cells
- periventricular = 3-5 cell wide zone adjacent to the third ventricle
- anterior = cranial to the compact part
- midlevel medial = located between the compact part and the periventricular zone at the mid level of the PVN
- posterior = located caudal to the compact part

Distribution of TRH-IR neurons in the PVN

TRH-IR neurons were observed in all parts of the PVN except in the periventricular zone. Moving from rostral to caudal portions of the PVN, TRH-containing neurons were observed in all three levels (anterior, mid and posterior levels), but the density of these cells was the highest at the anterior and mid levels of the PVN. The largest number of the detected TRH neurons was observed in the compact part of the PVN. The shape and size of the TRH neurons located in the compact and in the other parts of the PVN were similar (size of TRH neurons in midlevel medial part of the PVN vs. compact part (μm): 12.15 ± 0.05 vs. 12.26 ± 0.02 ; $P=0.31$).

Distribution of hypophysiotropic TRH neurons in the PVN

Fluoro-Gold accumulating in neuronal perikarya was readily visualized and had an inhomogeneous and punctuate appearance. Although the anterior part of the PVN contained a large number of TRH neurons, only very few were co-labeled with Fluoro-Gold. Similarly, none of the TRH neurons in the posterior part of the PVN contained Fluoro-Gold. Most double-labeled neurons were located in the compact part of the PVN.

Comparison between the distribution of hypophysiotropic TRH neurons and vasopressin and oxytocin neurons in the PVN

AVP and OT neurons were observed primarily in the compact part of the PVN, although scattered cells were also observed in the midlevel medial part of PVN. The size of magnocellular AVP neurons ($16.4 \pm 0.1 \mu\text{m}$) was significantly larger than the size of the TRH neurons ($p < 0.001$). Hypophysiotropic TRH neurons containing both Fluoro-Gold- and TRH-immunoreactivity were also primarily observed in the compact part of the PVN, and were intermingled with AVP and OT neurons. No co-localization of TRH and AVP or OT was observed in this region. In addition, no co-localization was observed in any other region of the PVN where OT and AVP were identified.

To further clarify the presence of magnocellular and parvocellular cells in the compact and midlevel medial parts of the PVN, histograms of the cell sizes were created using criteria for magnocellular neurons as $\geq 14 \mu\text{m}$ and parvocellular as $< 14 \mu\text{m}$. In the compact part, an approximately equal number of cells had less than $14 \mu\text{m}$ diameter ($49.3 \pm 0.9\%$) or $14 \mu\text{m}$ or greater diameter ($50.7 \pm 0.9\%$). In the midlevel medial part of PVN, the vast majority of cells were smaller than $14 \mu\text{m}$ ($96.0 \pm 1.2\%$) and only scattered cells had diameter $14 \mu\text{m}$ or greater ($4.4 \pm 1.2\%$).

Co-localization of CART and TRH in the neurons of the PVN

The localization of neurons co-synthesizing CART and TRH in the PVN of mice was similar to that of the TRH neurons accumulating Fluoro-Gold. Numerous CART-TRH double-labeled neurons were observed at the mid level of PVN in the compact part. Co-localization of CART and TRH was not detected in the posterior part of PVN, and only a few double-labeled cells were present in the anterior part. Co-localization of the two peptides was also detected in the axon terminals of the median eminence.

Determine the potential route of transport between the thyroid hormone activating tanycytes and hypophysiotropic TRH neuron

Presence of MCT8 in the hypophysiotropic axon terminals in the median eminence

To determine whether the hypophysiotropic terminals are capable of accumulating T3, the distribution of MCT8-immunoreactivity was studied in the median eminence. Intense and diffuse MCT8-immunoreactivity was observed in cell bodies and processes exhibiting the characteristic distribution and morphology of tanycytes. In addition, punctate MCT8-immunoreactivity was detected among the tanycyte processes in the external zone of the median eminence. Ultrastructural analysis of the MCT8-IR elements in the external zone of the median eminence demonstrated strong MCT8-immunoreactivity distributed uniformly in

the tanycyte processes. In addition, MCT8-immunoreactivity was also observed in axon terminals, where the silver grains focally accumulated in a segment of the axon varicosities in close proximity to the plasma membrane.

Co-localization of MCT8 and TRH in hypophysiotropic axon terminals

A series of double-labeling immunofluorescent staining for MCT8 and TRH demonstrated the presence of MCT8-IR puncta on the surface of the vast majority of TRH-containing axon varicosities in the external zone of the median eminence.

Understanding the mechanism of the melanocortin-resistance of hypophysiotropic TRH neurons during refeeding

AGRP- and α -MSH-IR innervation of TRH neurons

A dense network of both AGRP- and α -MSH-IR axons was observed in the PVN surrounding the TRH neurons. The density of the α -MSH-containing axons was slightly higher in the most anterior part of PVN, while the network of the AGRP-IR axons seemed to be denser in the posterior level of the PVN. In the same antero-posterior level, no difference was observed in the density of the α -MSH- and AGRP-IR axons in the medial and compact part of the PVN. Large number of AGRP- and α -MSH-IR axon varicosities formed juxtaposition with the perikarya and dendrites of the TRH neurons. In the mid level of PVN by confocal microscopic analyses an average of 30.9 ± 0.3 AGRP- and 19.3 ± 0.4 α -MSH-IR axon varicosities were found on the surface of perikarya and first order dendrites of TRH neurons.

The effect of fasting on the number of α -MSH- and AGRP-IR boutons on TRH neurons

Fasting caused a marked increase in the number of AGRP-immuno-labelled axon varicosities on the surface of TRH neurons (fasting vs. fed: 44.9 ± 0.3 vs. 30.9 ± 0.3 axon varicosities / TRH neurons; $P < 0.001$) and decrease in the number of α -MSH-IR boutons (fasting vs. fed: 13.6 ± 0.7 vs. 19.3 ± 0.4 axon varicosities / TRH neurons; $P < 0.001$) in contact with the TRH neurons in the PVN. Therefore, fasting resulted in a 2.07 fold increase in the ratio of AGRP- and α -MSH-IR varicosities forming contact with the TRH neurons (fasting vs. fed: 3.34 ± 0.2 vs. 1.61 ± 0.03 ; $P < 0.001$).

Comparison of the effect of 2h and 24h refeeding on the number α -MSH- and AGRP-IR boutons in contact with TRH neurons

Two hours after the start of refeeding, the number of AGRP-boutons on the surface of TRH neurons differed only slightly, but significantly from the fasted values (2h refed vs. fasted: 46.0 ± 0.3 vs. 44.9 ± 0.3 axon varicosities / TRH neurons; $P=0.018$). However, the number of AGRP-IR innervation of TRH neurons was markedly elevated compared to that in the fed animals (2h refed vs. fed: 46.0 ± 0.3 vs. 30.9 ± 0.3 axon varicosities / TRH neurons; $P<0.001$). Two hours after the onset of refeeding no significant alteration was observed in the α -MSH-innervation of TRH neurons compared to that observed in fasted animals (2h refed vs. fasted: 13.9 ± 0.8 vs. 13.6 ± 0.7 axon varicosities / TRH neurons; $P=0.746$). At this timepoint, the ratio of AGRP and α -MSH containing boutons was unchanged when it was compared to that observed in the fasted animals (2h refed vs. fasted: 3.33 ± 0.2 vs. 3.34 ± 0.2 ; $P=0.967$). In contrast, 24 hours after the start of food consumption a marked decrease was observed in the number of AGRP-IR axon varicosities on the TRH neurons compared to fasted animals (24h refed vs. fasted: 34.4 ± 0.1 vs. 44.9 ± 0.3 axon varicosities / TRH neurons; $P<0.001$), though this number was still slightly higher than it was observed in fed animals (24h refed vs. fed: 34.4 ± 0.1 vs. 30.9 ± 0.3 ; $P<0.001$). At this timepoint, the number of α -MSH-IR boutons in contact with TRH neurons was markedly increased compared to the fasted animals (24h refed vs. fasted: 20.9 ± 0.6 vs. 13.6 ± 0.7 axon varicosities / TRH neurons; $P<0.001$) and there was no significant difference between the α -MSH-IR innervation of TRH neurons in these mice and fed animals (24h refed vs. fed: 20.9 ± 0.6 vs. 19.3 ± 0.4 axon varicosities / TRH neurons; $P=0.153$). The ratio of the AGRP- and α -MSH-IR varicosities of TRH neurons was markedly lower than in fasted mice (24h refed vs. fasted: 1.64 ± 0.01 vs. 3.34 ± 0.2 ; $P<0.001$). In addition, no significant difference was observed in the ratio of AGRP- and α -MSH-IR innervation of TRH neurons compared to fed animals (24h refed vs. fed: 1.64 ± 0.01 vs. 1.61 ± 0.03 ; $P=0.866$).

The effect of leptin treatment on the fasting-induced rearrangement of α -MSH- and AGRP-innervation of TRH neurons

Leptin administration by subcutaneously implanted osmotic minipump completely prevented the fasting induced changes in the α -MSH-IR innervation of TRH neurons (leptin treated fasting vs. fasting: 20.5 ± 0.1 vs. 13.6 ± 0.7 axon varicosities / TRH neurons; $P<0.001$; leptin treated fasting vs. fed: 20.5 ± 0.1 vs. 19.9 ± 0.4 axon varicosities / TRH neurons; $P=0.178$) and markedly attenuated the fasting induced alteration in the number of AGRP-IR boutons on

the surface of these cells (leptin treated fasting vs. fasting 34.4 ± 0.1 vs. 44.9 ± 0.3 axon varicosities; $P < 0.001$; leptin treated fasting vs. fed: 34.4 ± 0.1 vs. 30.9 ± 0.3 axon varicosities / TRH neurons; $P < 0.001$). This treatment also prevented the fasting induced change in the ratio of AGRP- and α -MSH innervation of TRH neurons (leptin treated fasting vs. fasting: 1.67 ± 0.01 vs. 3.34 ± 0.02 ; $P < 0.001$; leptin treated fasting vs. fed: 1.67 ± 0.01 vs. 1.61 ± 0.03 ; $P = 0.939$).

Improve the method for combination of immunocytochemistry and Nissl-staining

Effects of RNase-free immunocytochemical method on the c-Fos immunostaining in the hypothalamus after refeeding

Two hours after refeeding, the hypothalamic nuclei including the ventral parvocellular subdivision of the vPVN showed identical distribution pattern of c-Fos-IR neurons as it was described earlier.

The RNase-free treatment did not alter the distribution of c-Fos immunoreactivity.

Analysis of the juxtaposition of NPY-IR varicosities and c-Fos-IR neurons in the vPVN after refeeding using standard immunocytochemical method combined with Nissl-counterstaining

Nissl-counterstaining after standard immunocytochemistry resulted in labeling of cell nuclei, but stained only very faintly the neuronal perikarya. Numerous NPY-IR fibers were detected in the vPVN around the c-Fos containing neurons. However, due to the very faint cytoplasmic staining, the extent of cytoplasm could not be detected, and therefore, it was not possible to determine the number of c-Fos-IR neurons contacted by NPY-IR varicosities.

Analysis of the juxtaposition of NPY-IR varicosities and c-Fos-IR neurons in the vPVN after refeeding using RNase-free immunocytochemical method combined with Nissl-counterstaining

After RNase-free immunocytochemistry, cresyl-violet dye stained not only the cell nuclei but also labeled the cytoplasm of neurons. This cytoplasmic staining facilitated the identification of the different subdivisions of the PVN and the correct location of labeled cell populations. In addition, the clear labeling of cytoplasm made the cell borders visible. c-Fos-IR neurons in the vPVN were contacted by numerous NPY-IR fibers. By quantification of the contacts, we have observed that $84.99 \pm 2.35\%$ of c-Fos-IR neurons were contacted by NPY-IR varicosities.

Conclusions

In summary, the organization of PVN in mice is markedly different from that observed in rats. The so called magnocellular part of this nucleus contains approximately equal number of parvo- and magnocellular neurons. Therefore, we suggest to call this part of the PVN compact part based on the high concentration of neurons in this division. The distribution of hypophysiotropic TRH neurons is also different in mice than in rats. These neurons are located exclusively in the mid level of PVN. Only a few hypophysiotropic TRH neurons were found in the anterior level of PVN, while these neuron type was absent from the posterior level of the nucleus. Interestingly, no hypophysiotropic TRH neuron was found in the periventricular zone of PVN of mice though numerous hypophysiotropic TRH neurons are located in this zone of PVN in rats. In mice, most of the hypophysiotropic TRH neurons are located in the compact part intermingled with magnocellular neurons, but no co-localization of TRH and AVP or OT was observed, and based on their size, all hypophysiotropic TRH neurons are parvocellular cells. The distribution of the hypophysiotropic and CART expressing TRH neurons overlap suggesting that hypophysiotropic TRH neurons express CART in mice similarly as it was observed in rats.

The presence of MCT8 thyroid hormone transporter on the terminals of hypophysiotropic TRH neurons in the median eminence suggests that these terminals can take up T3 from the extracellular space of the median eminence and likely transport it to the nucleus of hypophysiotropic TRH neurons. As the median eminence is located outside of the BBB and contains D2 expressing tanycytes, the origin of the T3 content of this brain region is unique: it derives from both the peripheral blood and the tanycytes. Therefore, the hypophysiotropic TRH neurons can be directly influenced by the changes of peripheral T3 concentration, but also by the activity of tanycytes that gives high flexibility to feedback regulation of TRH neurons.

In addition to the effects of fasting and leptin on the activity of the feeding related neurons of the arcuate nucleus, the nutritional signals may also influence the hypophysiotropic TRH neurons by inducing synaptic plasticity in the arcuato-paraventricular pathway. The fasting induced increase of the AGRP- and decrease of the α -MSH-innervation of TRH neurons may facilitate the fasting induced inhibition of the hypophysiotropic TRH neurons. Since this change of the innervation pattern lasts at least 2 hours after the onset of refeeding, it may contribute to the melanocortin-resistance of TRH neurons during this early phase of refeeding. 24 hours after the start of refeeding the ratio between the AGRP- and α -MSH-innervation of

TRH neurons reverts to fed level coincidently with the normalization of TRH expression. Leptin administration prevents the fasting-induced changes in the ratio between AGRP- and α -MSH-innervation of TRH neurons suggesting that leptin is the main factor that regulates the plasticity of the synaptic input of TRH neurons.

Our data demonstrate that the RNase contamination of materials used for immunocytochemistry contributes to the decrease of cytoplasmic labeling of neurons with basic dyes when Nissl staining is combined with immunocytochemistry. The application of RNase free techniques, therefore, can highly assist the detection of the cytoplasm with Nissl-staining and facilitate the examination of the neuronal inputs of neurons identified by their nuclear protein content.

List of publications

List of publications underlying the thesis

1. Kádár, A., Wittmann, G., Liposits, Z., Fekete, C. (2009) Improved method for combination of immunocytochemistry and nissl staining, *Journal of comparative neuroscience methods*. 184: (1) pp. 115-118.
2. Kádár, A., Sanchez, E., Wittmann, G., Singru, P., Füzesi, T., Marsili, A., Larsen, R., Liposits, Z., Lechan, R., Fekete, C. (2010) Distribution of hypophysiotropic thyrotropin-releasing hormone (TRH)-synthesizing neurons in the hypothalamic paraventricular nucleus of the mouse, *Journal of comparative neurology*. 518: pp 3948-3961
3. Kalló, I., Mohácsik, P., Vida, B., Zeöld, A., Bardóczi, Z., Zavacki, AM., Farkas, E., Kádár A., Hrabovszky, E., Arrojo e Drigo, R., Dong, L., Barna, L., Palkovits, M., Borsay, B.A., Herczeg, L., Bianco, A.C., Liposits, Z., Fekete, C., Gereben, B. (2012) A novel pathway regulates thyroid hormone availability in rat and human hypothalamic neurosecretory neurons, *PLoS One* 7: (6) Paper e37860. 16 p.

List of publications related to the subject of the thesis

1. Fekete, C., Freitas, B.C., Zeöld, A., Wittmann, G., Kádár, A., Liposits, Z., Christoffolete, M.A., Singru, P., Lechan, R.M., Bianco, A.C., Gereben, B. (2007) Expression patterns of WSB- ϵ and USP-33 underlie cell-specific post-translational control type 2 deiodinase in rat brain, *Endocrinology* 148: pp. 4865-4874
2. Fekete, C., Zséli, G., Singru, P., Kádár, A., Wittmann, G., Füzesi, T., El-Bermani, W., Lechan, R. (2012) Activation of anorexigenic POMC neurons during refeeding is independent of vagal and brainstem inputs, *Journal of neuroendocrinology* 24: (11) pp. 1423-1431
3. Sárvári, A., Farkas, E., Kádár, A., Zséli, G., Füzesi, T., Lechan, R., Fekete, C. (2012) Thyrotropin-releasing hormone-containing axons innervate histaminergic neurons in the tuberomammillary nucleus, *Brain research* 1488: pp. 72-80